Biochimie 94 (2012) 214–221

Contents lists available at SciVerse ScienceDirect

Biochimie

journal homepage: www.elsevier.com/locate/biochi

Research paper

Kinetic and *in silico* analysis of the slow-binding inhibition of human poly(A)-specific ribonuclease (PARN) by novel nucleoside analogues

Nikolaos Balatsos [a,**], Dimitrios Vlachakis [b], Vassiliki Chatzigeorgiou [a], Stella Manta [a], Dimitri Komiotis [a], Metaxia Vlassi [b], Constantinos Stathopoulos [c,*]

[a] Department of Biochemistry & Biotechnology, University of Thessaly, 26 Ploutonos st., 41 221 Larissa, Greece
[b] Institute of Biology, National Centre for Scientific Research "Demokritos", 15 310 Aghia Paraskevi, Attikis, Greece
[c] Department of Biochemistry, School of Medicine, University of Patras, 1 Asklipiou st., 26 504 Rio-Patras, Greece

ARTICLE INFO

Article history:
Received 23 June 2011
Accepted 17 October 2011
Available online 24 October 2011

Keywords:
PARN
Deadenylation
Slow-binding inhibition
Nucleoside analogues

ABSTRACT

Poly(A)-specific ribonuclease (PARN) is a 3′-exoribonuclease that efficiently degrades poly(A) tails and regulates, in part, mRNA turnover rates. We have previously reported that adenosine- and cytosine-based glucopyranosyl nucleoside analogues with adequate tumour-inhibitory effect could effectively inhibit PARN. In the present study we dissect the mechanism of a more drastic inhibition of PARN by novel glucopyranosyl analogues bearing uracil, 5-fluorouracil or thymine as the base moiety. Kinetic analysis showed that three of the compounds are competitive inhibitors of PARN with K_i values in the low μM concentration and significantly lower (11- to 33-fold) compared to our previous studies. Detailed kinetic analysis of the most effective inhibitor, the uracil-based nucleoside analogue (named U1), revealed slow-binding behaviour. Subsequent molecular docking experiments showed that all the compounds which inhibited PARN can efficiently bind into the active site of the enzyme through specific interactions. The present study dissects the inhibitory mechanism of this novel uracil-based compound, which prolongs its inhibitory effect through a slow-binding and slow-release mode at the active site of PARN, thus contributing to a more efficient inhibition. Such analogues could be used as leading compounds for further rationale design and synthesis of efficient and specific therapeutic agents. Moreover, our data reinforce the notion that human PARN can be established as a novel molecular target of potential anti-cancer agents through lowering mRNA turnover rates.

1. Introduction

A critical step in mRNA degradation is the removal of the poly(A) [1]. The process is catalyzed by deadenylases both in the nucleus and in the cytoplasm [2,3]. Among those enzymes, poly(A)-specific ribonuclease (PARN) holds a key role both in development [3] and in mRNA 3′-end processing upon DNA-damaging conditions [4]. PARN is a dimeric enzyme where each subunit is composed of three characteristic structural motifs and belongs to the DEDD family of nucleases. It is the only known deadenylase, so far to interact both with the 5′-cap structure and the poly(A) tail [5–7]. This interaction regulates PARN activity possibly by preventing the cap-binding of the translation initiation factor eIF4E, and/or by competing with the nuclear cap-binding complex subunit CBP80 [8,9]. It is also known that poly(A)-binding protein C (PABPC) inhibits PARN activity, probably through binding and interfering with the poly(A) substrate [10,11]. On the other hand, PARN-mediated poly(A) degradation is promoted by AU-rich elements (AREs) and ARE-associated proteins [6,12–14].

PARN can be modulated by small compounds, such as aminoglycoside antibiotics [15], and natural purine nucleotides that inhibit its degrading activity [16,17]. More recently, work from our group has shown that PARN can be effectively inhibited by a novel family of synthetic nucleoside analogues, which are based on glucopyranosyl rings as the sugar moiety [18]. These compounds have been evaluated for their efficient anti-cancer and anti-viral potency when tested in cell cultures. Such novel nucleoside analogues have emerged as important therapeutic agents for the development of anti-viral and antitumour drugs [19–21]. Various novel unsaturated ketopyranonucleosides [20,22–26] have been developed and

Abbreviations: PARN, poly(A)-specific ribonuclease; U or FU, uracil or 5-fluorouracil, respectively; U1, [1-(3′-deoxy-3′-fluoro-β-D-glucopyranosyl)] uracil; FU1, [1-(3′-deoxy-3′-fluoro-β-D-glucopyranosyl)] 5-fluorouracil.

* Corresponding author. Tel.: +30 2610 997932; fax: +30 2610 969167.
** Corresponding author. Tel.: +30 2410 565261; fax: +30 2410 565290.
E-mail addresses: balatsos@bio.uth.gr (N. Balatsos), cstath@med.upatras.gr (C. Stathopoulos).

0300-9084/$ – see front matter © 2011 Elsevier Masson SAS. All rights reserved.
doi:10.1016/j.biochi.2011.10.011

have been shown to effectively inhibit PARN, which represents a promising molecular target [18]. Based on the properties of those nucleosides analogues, and the significance of PARN for the regulation of the mRNA lifecycle, we have been actively engaged in the development and the study of various unsaturated ketopyranonucleosides and their inhibitory effect on PARN activity.

In the present study, we investigated the inhibitory effect of novel glycopyranosyl nucleosides on human PARN activity, through detailed kinetic analysis and molecular docking. After testing several compounds, we concluded that the most effective inhibitor which is based on uracil (U1, Table 1) represents a less bulky, less conjugated compound with much more flexible core and increased potency when compared to the adenosine- and cytosine-based compounds that we have tested and characterized so far [18]. These compounds represent drastic molecules at the μM range (11- to 33-fold more effective when compared to our previous studies) that act through a mechanism that allows slow-binding and slow-release on the active site of the enzyme. Therefore they enhance significantly their drastic effect since they prolong their inhibitory interactions with the active site of the enzyme. Both our biochemical and *in silico* analysis suggest that the effective inhibition by slow-binding nucleoside analogues represents an adequate mechanism of PARN inhibition at least *in vitro*. Since human PARN represents a suitable and effective target for inactivation and for the development of anticancer compounds, our results provide substantial evidence for promising *in vivo* trials of such compounds that could effectively inhibit PARN and thus, providing the means to lowering mRNA turnover rates in de-regulated cell lines.

2. Materials and methods

2.1. Materials

All chemicals including purine ribonucleotides and deoxynucleotides, methylene blue, polyadenylic acid potassium salt (average size 300 adenosines, A_{300}) and polyuridine acid potassium salt (average size 300 uracils, U_{300}) were from Sigma-Aldrich.

2.2. Synthesis of nucleoside analogues

The desired fluoro-pyranosyl nucleosides were synthesized by implementing the Vorbruggen glycosylation reaction, adapted into a one-step 5 min/130 °C microwave (MW)-assisted reaction, followed by subsequent deprotection. As an extension of a methodology recently developed by our group for the synthesis of fluorinated nucleosides [20,24,25], we found that it can be more easily prepared in an one-step reaction using elevated temperatures generated by microwave heating and we observed that the glycosylation reactions could be conducted satisfactorily in 5 min at 130 °C. Using this approach, reaction of 1,2,4,6-tetra-*O*-acetyl-3-deoxy-3-fluoro-glucopyranose [20] with uracil, 5-fluorouracil, thymine, N^4-benzoyl cytosine, and N^6-benzoyl adenine under MW irradiation at 130 °C for 5 min gave the protected 1-(2,4,6-tri-*O*-acetyl-3-deoxy-3-fluoro-β-D-glucopyranosyl) nucleosides, in the presence of trimethylsilyltrifluoromethane-sulfonate and tin chloride, respectively. Deacetylation of uracil, 5-fluorouracil and thymine derivatives with ammonia in methanol afforded nucleosides [1-(3′-deoxy-3′-fluoro-β-D-glucopyranosyl)] uracil (U1), [1-(3′-deoxy-3′-fluoro-β-D-glucopyranosyl)] 5-fluorouracil (FU1) and [1-(3′-deoxy-3′-fluoro-β-D-glucopyranosyl)] thymine (T1), while deprotection of N^4-benzoyl cytosine and N^6-benzoyl adenine derivatives with NaOH–ethanol–pyridine, yielded benzoylated analogues A2 and A6. The chemical and physical properties of the fluoro-pyranosyl nucleosides were in agreement with previous data [20,24,25]. The nomenclature and the chemical formulae of the compounds used in the present study are shown in Table 1.

2.3. Purification of recombinant PARN, activity assays and kinetic analysis

The plasmid encoding full-size 74 kDa human PARN (for expression of N-terminal His_6-tagged polypeptide) was transformed into BL21(DE3) cells to express the recombinant protein as described previously [27].

The enzymatic activity was determined by the methylene blue assay as described before [28]. Methylene blue buffer was prepared by dissolving 1.2 mg methylene blue into 100 ml Mops buffer (0.1 M MOPS-KOH, pH 7.5, 2 mM EDTA). The standard reaction buffer contained 50 mM KH_2PO_4/K_2HPO_4 (pH 7.0), 1.5 mM $MgCl_2$, 100 mM KCl, 0.2 mM EDTA, 0.25 mM DTT, 10% (v/v) glycerol and 0.1 U of RNasin. All analogues were dissolved in reaction buffer prior to use. The reactions were performed using 10–15 μM of recombinant PARN. To evaluate the effect of Mg(II) ions on PARN activity in the presence of the analogues, deadenylation assays were performed as described above. The concentration of Mg(II) varied from 0.15 mM to 15 mM (10-fold below and above the standard assay concentration). For kinetic analysis, the substrate concentration [poly(A)] varied from 70 to 600 μM [17], and from 10 to 500 μM for the compounds tested. The final reaction volume was 100 μl and the reaction was performed at 30°C for 10 min. The reaction was terminated by mixing the reaction solution with 900 μl methylene blue buffer and the mixed solution was incubated at 30 °C for another 15 min in the dark in a water bath. The absorbance at 662 nm of 1 ml sample was measured on a Spectronic Genesys 20 spectrophotometer.

2.4. Molecular docking

The Schrödinger suite of programs and the program Glide[1] (grid-based ligand docking with Energetics) was used for the molecular docking experiments. The Maestro program[2] was used for molecular building and coordinate preparation prior to docking. The coordinates of the crystal structure of PARN (Protein Data Bank accession code 2A1R) were used as the receptor and the structure was prepared using the Protein Preparation Wizard[3] module of Maestro. All crystallographic water molecules were removed from the coordinate file prior to docking. Hydrogen atoms and partial charges were added to the enzyme and the initial structure was energy minimized using the OPLS-AA force field [29]. For docking, the scoring grid file was generated through the Glide Receptor Grid Preparation module, using the same active site of PARN as previously [18]. A docking box of 40 × 40 × 40 points with a van der Waals scaling factor of 1.0, was placed around the active site of the protein, for this purpose the compound optimization module of Maestro, LigPre[4] was used to prepare the ligand database. For each compound, 32 stereoisomers were generated and their 3D-structure was minimized using the OPLS-AA force field. The best three conformations of each compound were kept for docking. The Glide XP (extra precision) method [30] was employed for all docking calculations.The maximum number of poses was set to 1000 and the number of runs was set to 1. The best-docked pose for each

[1] Glide, version 5.5, Schrödinger, LLC, New York, NY, 2009.
[2] Maestro, version 9.0, Schrödinger, LLC, New York, NY, 2009.
[3] Schrödinger Suite 2009 Protein Preparation Wizard; Epik version 2.0, Schrödinger, LLC, New York, NY, 2009; Impact version 5.5, Schrödinger, LLC, New York, NY, 2009; Prime version.
[4] LigPrep (LigPrep, version 2.3, Schrödinger, LLC, New York, NY, 2009).

Table 1
Synthetic nucleosides used in the present work and inhibition constants.

Nucleoside		K_i, μM	Chemical formula
Nomenclature	Abbreviation		
1-(3′-deoxy-3′-fluoro-β-D-glucopyranosyl) uracil	U1	19 ± 5	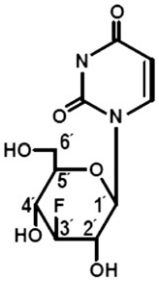
1-(3′-deoxy-3′-fluoro-β-D-glucopyranosyl) 5-fluorouracil	FU1	98 ± 12	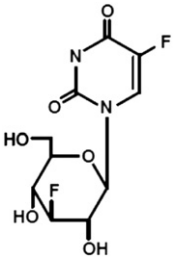
1-(3′-deoxy-3′-fluoro-β-D-glucopyranosyl) thymine	T1	135 ± 18	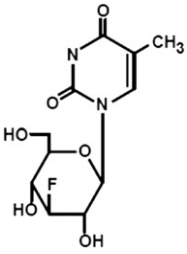
9-(3′,4′, dideoxy-3′-fluoro-β-D-glucopyranosyl)-N^6-benzoyl adenine	A2	510 ± 52[a]	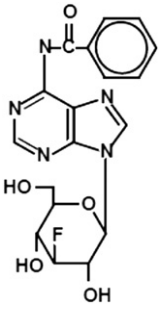
1-(3′,4′, dideoxy-3′-fluoro-β-D-glucopyranosyl)-N^4-benzoyl adenine	A6	210 ± 45[a]	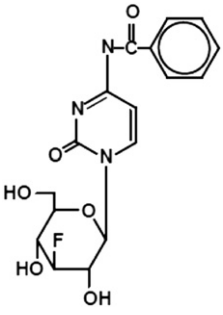
3-deoxy-3-fluoro-glucopyranose	B6	ND[a]	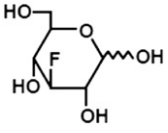

[a] Data from [18].

compound was selected as the one with the lowest Glide Score [30]; the more negative the Glide Score the more favourable the binding.

3. Results

3.1. U1, FU1 and T1 are competitive inhibitors of PARN

Recently, we examined the effect of several fluoro-pyranosyl nucleosides with established anti-cancer and anti-viral activity, as potential inhibitors of human PARN [18]. The inhibition of PARN by compounds bearing adenine has been already established from our previous studies and therefore we extended our survey on novel analogues bearing uracil and thymine as the base moiety in a survey of improved inhibitors. It has been reported that although PARN degrades preferably poly(A) tails *in vivo*, it can also recognise uracil and can degrade poly(U), albeit approximately 10-fold less effectively than poly(A) [31].The novel analogues bear modified sugar moiety to fit into the active site, as we have previously predicted *in silico* [18]. After initial screening for PARN inhibition, we performed detailed kinetic analysis which revealed that three compounds U1, FU1 and T1 behave as more efficient competitive inhibitors of PARN *in vitro* (Fig. 1) compared to the compounds A2 and A6 that exhibit the strongest inhibition (11- to 33-fold) among the analogues bearing adenine [18]. The calculated K_i values were 20 μM for U1, 98 μM for FU1 and 135 μM for T1. The compound B6 (3-deoxy-3-fluoro-glucopyranose), which contains only the same sugar ring without the base moiety, showed no inhibition and in the subsequent analysis was used as the negative control (Table 1). Our data show that glucopyranosyl nucleoside analogues with uracil or thymine as the base moiety are suitable suppressors of PARN activity and act as competitive inhibitors. In particular U1 inhibits PARN more efficiently than other analogues tested.

3.2. U1 is a slow-binding inhibitor of PARN

The fact that the U1 is an efficient inhibitor of PARN and taking into account that PARN degrades *in vitro* poly(U) in a much slower rate than it degrades poly(A) [31], prompted us to examine the inhibitory mechanism in more detail. When the initial rates of the reactions in the presence of increasing amounts of U1 were plotted near the origin, the slopes of the progress curves changed rapidly, implying slow-binding inhibition [32]. The time-dependent inhibition of U1 is illustrated in Fig. 2A, showing the first-order time plots of poly(A) degradation in the presence or absence of the compound. The control reaction (absence of inhibitor) is linear, therefore the analysis of the inhibition is analysed by fitting progress curves to equation (1) (termed "burst equation") [32–35]:

$$[P] = \frac{v_s t + (v_0 + v_s)\left(1 - e^{-k_{obs}t}\right)}{k_{obs}} \quad (1)$$

where, [*P*] is the concentration of the product at time *t*, v_o and v_s are the initial and steady-state rates, and k_{obs} is the observed rate constant, or the exponential decay constant (s^{-1}) for the approach to the steady-state final rate [34]. For PARN activity assay the calculations are based on the degradation rate of the substrate.

In order to further dissect the mechanism of inhibition and determine whether U1 acts as rapidly or slowly reversible inhibitor, we used a preincubation/dilution assay [36]. In brief, PARN was pre-incubated with U1 for 60 min at 10-fold its K_i value (200 μM) leading to saturation of the active sites. The pre-incubated mixture was then

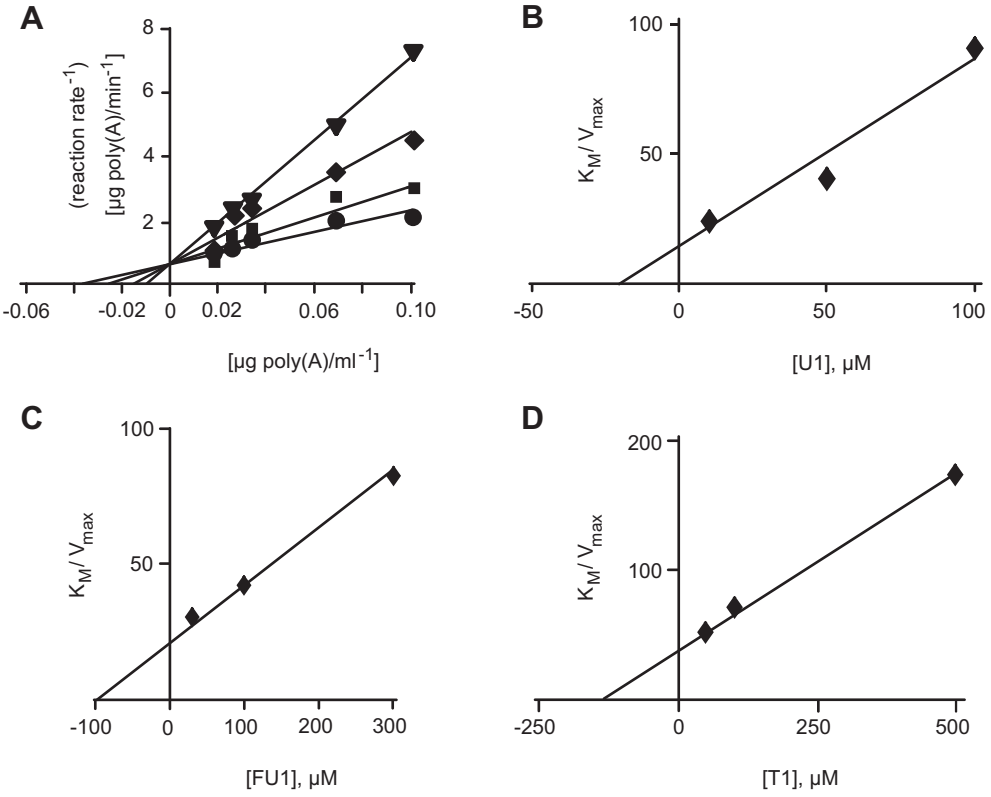

Fig. 1. Inhibition of PARN activity by novel nucleoside analogues. Double reciprocal plot 1/v versus 1/[substrate] for PARN activity in the presence of U1 (A). The U1 concentrations were 0 mM (circle), 0.010 mM (square), 0.050 mM (rhombus) and 0.1 mM (inverted triangle). The representative slopes (K_M/V_{max}) of the double reciprocal plots versus the nucleoside concentration for U1 (B), FU1 (C) and T1 (D) are shown.

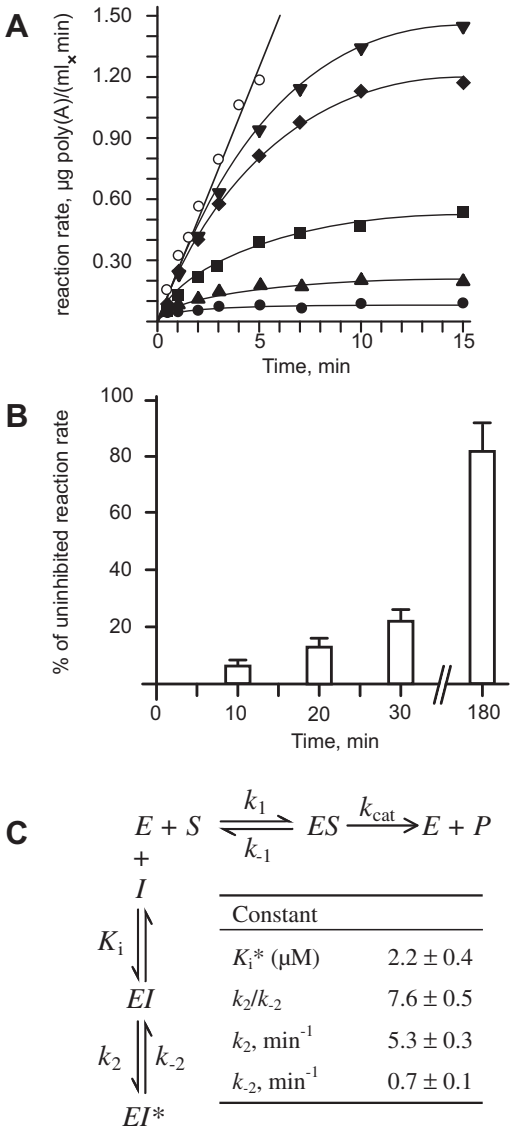

Fig. 2. A. Reaction progress curves in the presence of increasing concentrations of U1. Poly(A) degradation was monitored in the presence of 0 mM (open circle), 0.01 mM (inverted triangle), 0.025 mM (rhombus), 0.10 mM (square), 0.25 mM (triangle) and 1 mM (filled circle) of U1. B. Reversibility data for U1. PARN (0.07 μg/ml) was pre-incubated with 0.2 mM U1 for 60 min at 37 °C. The mixture was then diluted 100-fold into deadenylation assay mixture containing 7 μg poly(A)/ml. Reaction rates were monitored for 30 min further and expressed as percentage of the rates of the uninhibited (control) reaction. C. Proposed kinetic scheme for slow-binding inhibition of PARN by U1 including the calculated equilibrium and kinetic constants of PARN inhibition.

diluted 100-fold into the deadenylation assay mixture [containing 7 μg poly(A)/ml] and the activity rates were monitored for 30 min further and compared to the rates of the control reaction. A rapidly reversible inhibitor should dissociate from the enzyme to restore more than approximately 90% of activity [36]. Fig. 2B summarizes the results of the preincubation/dilution assay. The comparison of the pre-incubated and uninhibited reactions revealed that upon 100-fold dilution of the pre-incubated mixture of PARN and U1 into substrate-containing assay mixture, 7% of the enzymatic activity was restored after 10 min and 20% of the enzymatic activity was restored after 30 min. This observation shows that U1 is released from the enzyme–inhibitor complex, albeit in a very slow rate. Moreover, as mentioned above, the threshold for a recovered enzymatic activity in the presence of a rapidly reversible inhibitor is above 90% at the same time period, a value that could not be observed for U1. Actually, when we prolonged the assay time we could observe a very slow restoration of PARN activity (up to 80%) after 180 min (3 h) (Fig. 2B). These results strongly suggest that U1 is indeed a slowly reversible inhibitor of PARN and the binding of U1 into the active site of PARN is very stable.

Based on both the time-dependent inhibition of PARN by U1 and the preincubation assay, a kinetic model that describes with accuracy the inhibition of PARN by U1 is proposed (Fig. 2C), together with the respective kinetic data for each step. The non-covalent *EI* complex (PARN-U1) is rapidly formed followed by a slower step, where it is transformed to the more stable *EI** complex. In this process, K_i represents the equilibrium constant for the first step, K_i^* the overall dissociation constant and k_2, k_{-2} the interconversion rate constants [32]. At each concentration of U1, the k_{obs} values were determined for the initial (k^0_{obs}) and close to the steady-state (k^s_{obs}) according to equation 2:

$$\ln \frac{100}{100 - x} = k_{obs} \cdot t \qquad (2)$$

where, x is the percent of the poly(A) bound on PARN and t is the reaction time (Equation. (1a)) [37]. The double reciprocal plots of k^0_{obs} and k^s_{obs} versus several substrate concentrations are shown in Fig. 3 (A and B respectively), and show that the type of inhibition is competitive, as expected from the analysis using the initial rates shown in Fig. 1A. In addition, the slopes of the lines were reploted versus increasing U1 concentrations (Fig. 3C). Both replots are linear and meet the vertical axis at the same point, which coincides with the point of the corresponding control experiment ([U1] = 0 μM). The linearity of the replot also confirms the competitive mode of inhibition [40]. Both lines shown in Fig. 3C when extrapolated meet the horizontal axis at 19.4 and 2.2 μM, representing K_i and the overall dissociation constant K_i^*, respectively. The isomerisation constant, k_2/k_{-2} can be determined according to equation (3) [32,37] and equals to 7.6. Finally, the apparent association rate constant $(k_2 + k_{-2})/K_i$, of U1 binding, can be calculated and equals to 5.2×10^3 M^{-1} s^{-1}. This value is much lower than 10^6 M^{-1} s^{-1}, which is considered the upper limit value for the classification of a compound as slow-binding inhibitor [33,37].

$$K_i^* = \frac{K_i}{1 + \frac{k_{+2}}{k_{-2}}} \qquad (3)$$

Thus, our detailed kinetic analysis, show that compound U1 behaves as a slow-binding inhibitor of PARN. The overall dissociation constant K_i^* value is 10-fold lower than the K_i value (~2 μM versus 20 μM) indicating that *EI** complex is more stable than *EI* complex (Fig. 2C). None of the additional compounds tested in this work (FU1, TI or B6) behaved as slow-binding inhibitor of PARN.

Although poly(U) is not the natural substrate of PARN *in vivo*, it can be degraded by PARN *in vitro* [31]. Initial experiments were performed also using poly(U) as substrate (data not shown). We observed elevated K_M value for poly(U) and slow reaction rate, in agreement with current reports. In addition, the V_{max} value was unaffected. Based on the above, we concluded that using poly(A) as substrate is more appropriate because it is the natural substrate of PARN and it can be used in reduced amounts (comparing the K_M values). The use of either poly(A) or poly(U), does not significantly alter the kinetic behaviour (and thus the kinetic data) of the compounds tested in the present work (data not shown).

Biochemical studies have shown that Mg(II) ions are necessary for PARN activity at least *in vitro* [11,38]. We have previously

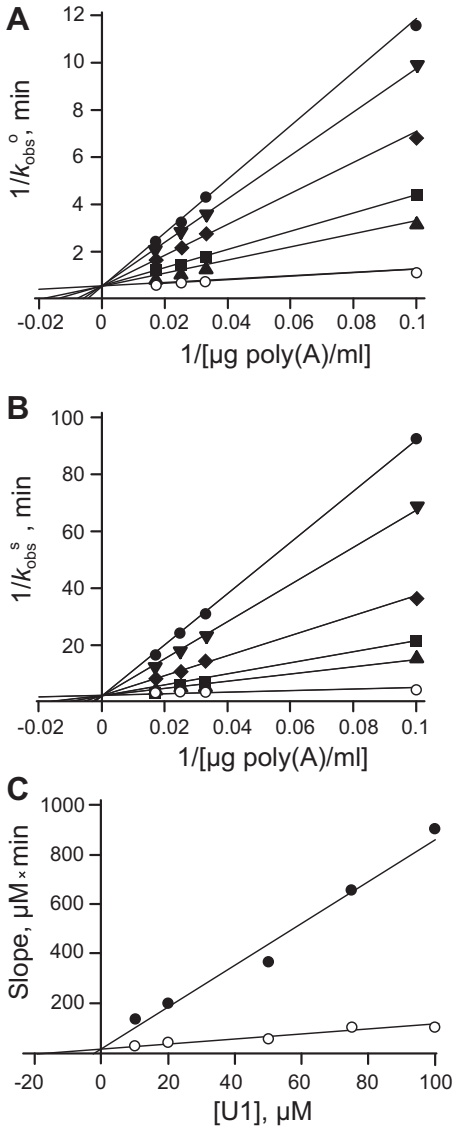

Fig. 3. Double reciprocal plots for PARN inhibition by U1. Panels A and B represent data collected from the early ($t < 30$ s) and the late phases ($t > 5$ min) of progress curve plots, respectively. U1 concentrations were 0 mM (open circle), 0.01 mM (triangle), 0.025 mM (square), 0.10 mM (rhombus), 0.25 mM (inverted triangle) and 1 mM (filled circle) of U1. C. Slopes of the double reciprocal plots versus U1 concentration (data of the double reciprocal plots were obtained from A and B). The replot represents the slopes of the lines from the early phase (filled circle) and late phase (open circle) from progress curves as shown in A and B, respectively. The linearity of the slope replots confirms the competitive behavior of U1.

reported that increased Mg(II) concentrations could release the inhibitory effect by natural di- and tri-phosphate nucleotides but not the inhibition by mono-phosphate nucleotides [17]. In addition, we have reported that inhibition of PARN by synthetic glucopyranosyl nucleosides is independent of the local Mg(II) concentration and the effect of these compounds can not be deprived by altering Mg(II) levels [18]. To exclude the possibility that the observed PARN inhibition could be rescued in the presence of Mg(II) excess, we performed deadenylation assays in the presence of Mg(II)concentrations varying approximately 10-fold below and above the concentration of the standard assay conditions, as described previously [18].In the present study, we verified that inhibition of PARN by either U1, FU1 or T1 was unaltered under all the Mg(II) concentrations tested (data not shown), although Mg(II) ions are important for enzymatic activity.

3.3. Molecular docking of U1, T1 and FU1 in the active site of PARN

To shed light on the binding mode of the inhibitory compounds that were tested, we performed *in silico* molecular docking experiments using the information from known crystal structure of a truncated form of PARN [44]. The best-docked conformation of compounds U1, FU1 and T1, as indicated by the lowest Glide Score for each compound, is shown in Fig. 4. The binding orientation of U1 in the active site of PARN (Fig. 4A) is optimal; the establishment of a hydrogen bond between the −OH group on the sugar C-2′ and Glu30 optimises the geometry of the other two −OH groups of the sugar ring to donate electrons to two of the Asp residues of the catalytic triad (Asp292 and Asp28). Moreover, one of the =O atoms on the phenyl ring interacts weakly with the backbone of Phe31, further stabilising and defining the binding mode of U1 within the active site of PARN, away from Phe115 (Fig. 4A). On the contrary, the methyl group that has been added to the base moiety of the compound T1 is attracted by a hydrophobic pocket formed by residues Phe155, Leu116 and Ser112 (Fig. 4B). Only one of the three −OH groups on the sugar ring of T1 interacts with Asp382 residue of the catalytic triad suggesting that this compound may be a less potent inhibitor of PARN compared to U1. This prediction is in agreement with our kinetic data, which show a higher K_i value for T1 compared to U1 (Table 1). On the other hand, the −OH group on the C-2′ atom of FU1 is again hydrogen bonded to Glu30 (Fig. 4C), as in the case of the U1 compound. However, a new hydrogen bond between one of the sugar's −OH groups and Asn288, slightly tilts the docking axis of FU1 offset. This orientation allows only one of the three −OH groups of the sugar moiety to interact with only one residue of the catalytic triad (Asp292). It is strongly suggested that the hydrogen bonding to Asn288 and the slight tilt of the axis of this compound are responsible for the lower inhibitory effect of FU1 compared to U1.

4. Discussion

Few are known about the biological significance of PARN. Recently, (and interestingly) PARN was reported to be involved in the late cytoplasmic cell-cycle checkpoint control through a mechanism that regulates 3′ end processing in response to DNA damage [39]. It has been demonstrated that PARN interacts with CstF-50, a factor involved in mRNA maturation and DNA repair, while the tumour-suppressor BARD1 strongly activates deadenylation by PARN in the presence of CstF-50. PARN along with the CstF/BARD1 participates in the regulation of endogenous transcripts under DNA-damaging conditions. All those novel evidence pinpoint PARN as a key player in a concerted and dynamic network between factors involved in mRNA maturation, degradation and tumour-suppression to prevent the expression of prematurely terminated messages, thus contributing to control of gene expression [4]. It is now evident that PARN is involved in cell-cycle checkpoint control. Besides the two well-established protein kinase-signalling units that modulate the key elements of checkpoint control [40], a recently characterized kinase pathway, p38/MK2, elicits checkpoint arrest [41–43].

Chemically stable enzyme inhibitors have received increasing attention in the design of drugs due to their potential for potency and selectivity. A slow rate of dissociation is important in drug design, since it is expected to enhance the effectiveness of the inhibitor. This quest for new compounds has led to the development of many potent, reversible inhibitors. A key characteristic of slow-binding inhibitors is that they do not rapidly establish equilibrium with their target enzymes relative to enzymatic turnover of substrate and exhibit a time-dependent inhibition following complex kinetics [32–35]. Human PARN represents a potential target for drug

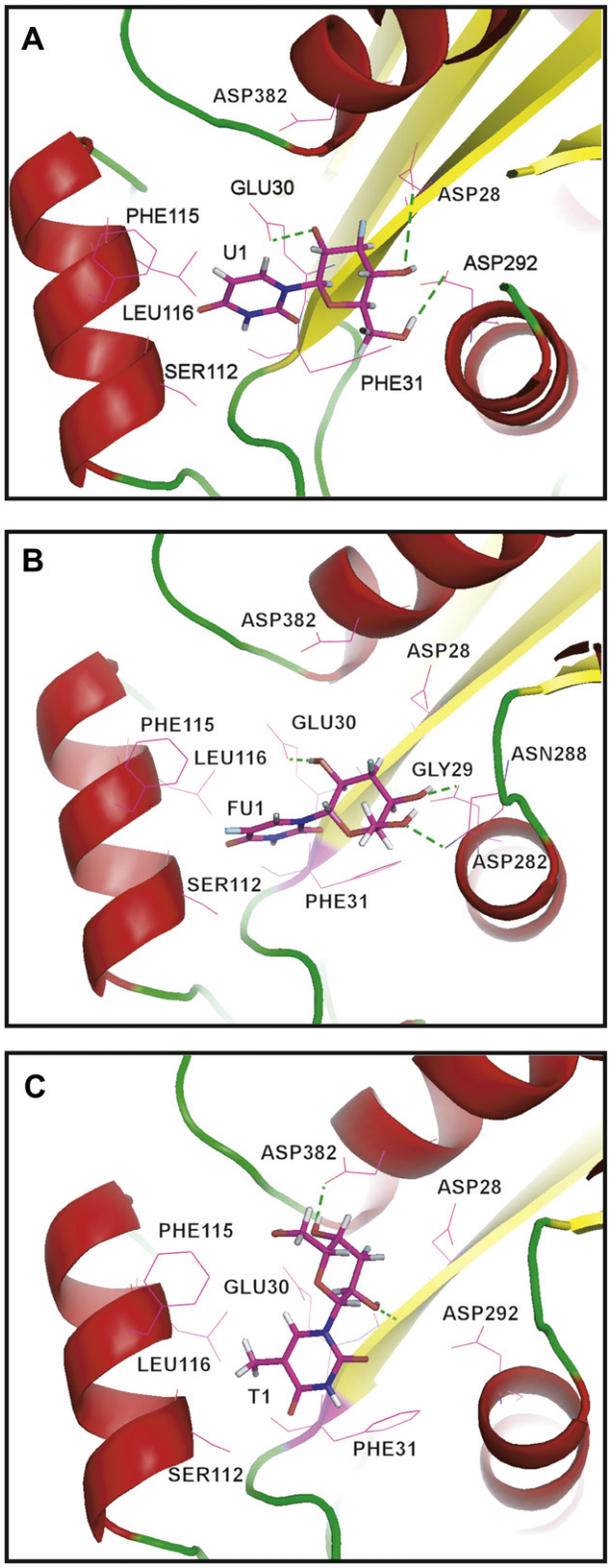

Fig. 4. Interactions between the active site of PARN and compounds U1 (A), FU1 (B) and T1 (C). 3D-models of the binding mode of the compounds into the active site of PARN as revealed by molecular docking experiments. Important residues of PARN, including Phe115, are shown in lines and labelled. Green dotted lines indicate hydrogen bonding between receptor and compound. The figure was made using Pymol.(For interpretation of the references to colour in this figure legend, the reader is referred to the web version of this article.)

development that has not been extensively studied so far. We have shown that fluoro-pyranosyl nucleosides with cytosine or modified adenine as the base moiety behave as competitive inhibitors of PARN and herein we report the mechanism of improved and drastic inhibitors of the enzyme's activity, based on both structural and biochemical analyses. Preliminary deadenylation assays revealed that the compounds U1, FU1 and T1 could efficiently inhibit PARN. Kinetic analysis showed that these compounds behave as competitive inhibitors, while the K_i values are significantly improved when compared to our previous report (summarized in Table 1) [18]. The preliminary analysis also showed that the inhibition of PARN by U1 was time-dependent. In-depth kinetic analysis revealed that U1 behaved as slow-binding competitive inhibitor. It should be noted that a slow-binding inhibitor that conform to this mechanism (such as U1) display a potential clinical advantage. In contrast to classic inhibitors, its effectiveness is not abolished by increased substrate concentration through feedback inhibition mechanism [33,34].

The higher potency of U1 can be also explained from the molecular docking analysis, which outlines the accommodation of U1 into the active site of PARN. It has been previously described that Phe115 is a key residue in the 3D-structure of PARN [18,44]. The side-chain of this residue may establish π-stacking interactions with any compound with conjugated enough base moieties, which compete the hydrogen bonding interactions of the −OH groups on the sugar moiety of the compounds with the Asp members of the catalytic triad. Therefore it appears that the stronger the interaction with Phe115, the weaker the interactions of the compound with the catalytic triad. U1 forms hydrogen bonds with most of the Asp residues of the active site than any other compound in Table 1, while at the same time does not form and is not able to form any π-stacking with Phe115 (Fig. 4).

Taken together, our kinetic and molecular docking data suggest that the uracil-based U1 compound is a novel efficient slow-binding inhibitor of PARN. This feature of U1 allows a stable and prolonged interaction with the active site of PARN [31,38]. Such molecules could represent promising leading compounds for the development of novel, effective and specific anti-cancer agents, both *in vitro* and *in vivo*.

References

[1] N.L. Garneau, J. Wilusz, C.J. Wilusz, The highways and byways of mRNA decay, Nat. Rev. Mol. Cell Biol. 8 (2007) 113–126.
[2] A.C. Goldstrohm, M. Wickens, Multifunctional deadenylase complexes diversify mRNA control, Nat. Rev. Mol. Cell Biol. 9 (2008) 337–344.
[3] J.H. Kim, J.D. Richter, Opposing polymerase-deadenylase activities regulate cytoplasmic polyadenylation, Mol. Cell 24 (2006) 173–183.
[4] M.A. Cevher, X. Zhang, S. Fernandez, S. Kim, J. Baquero, P. Nilsson, S. Lee, A. Virtanen, F.E. Kleiman, Nuclear deadenylation/polyadenylation factors regulate 3' processing in response to DNA damage, EMBO J. 29 1674–1687.
[5] E. Dehlin, M. Wormington, C.G. Körner, E. Wahle, Cap-dependent deadenylation of mRNA, EMBO J. 19 (2000) 1079–1086.
[6] M. Gao, C.J. Wilusz, S.W. Peltz, J. Wilusz, A novel mRNA-decapping activity in HeLa cytoplasmic extracts is regulated by AU-rich elements, EMBO J. 20 (2001) 1134–1143.
[7] J. Martinez, Y.G. Ren, P. Nilsson, M. Ehrenberg, A. Virtanen, The mRNA cap structure stimulates rate of poly(A) removal and amplifies processivity of degradation, J. Biol. Chem. 276 (2001) 27923–27929.
[8] N.A. Balatsos, P. Nilsson, C. Mazza, S. Cusack, A. Virtanen, Inhibition of mRNA deadenylation by the nuclear cap binding complex (CBC), J. Biol. Chem. 281 (2006) 4517–4522.
[9] R. Seal, R. Temperley, J. Wilusz, R.N. Lightowlers, Z.M. Chrzanowska-Lightowlers, Serum-deprivation stimulates cap-binding by PARN at the expense of eIF4E, consistent with the observed decrease in mRNA stability, Nucleic Acids Res. 33 (2005) 376–387.
[10] M. Gao, D.T. Fritz, L.P. Ford, J. Wilusz, Interaction between a poly(A)-specific ribonuclease and the 5' cap influences mRNA deadenylation rates in vitro, Mol. Cell 5 (2000) 479–488.
[11] C.G. Körner, E. Wahle, Poly(A) tail shortening by a mammalian poly(A)-specific 3'-exoribonuclease, J. Biol. Chem. 272 (1997) 10448–10456.
[12] R. Gherzi, K.Y. Lee, P. Briata, D. Wegmuller, C. Moroni, M. Karin, C.Y. Chen, A KH domain RNA binding protein, KSRP, promotes ARE-directed mRNA

turnover by recruiting the degradation machinery, Mol. Cell 14 (2004) 571–583.
[13] W.S. Lai, E.A. Kennington, P.J. Blackshear, Tristetraprolin and its family members can promote the cell-free deadenylation of AU-rich element-containing mRNAs by poly(A) ribonuclease, Mol. Cell. Biol. 23 (2003) 3798–3812.
[14] H. Tran, M. Schilling, C. Wirbelauer, D. Hess, Y. Nagamine, Facilitation of mRNA deadenylation and decay by the exosome-bound, DExH protein RHAU, Mol. Cell 13 (2004) 101–111.
[15] Y.G. Ren, J. Martinez, L.A. Kirsebom, A. Virtanen, Inhibition of Klenow DNA polymerase and poly(A)-specific ribonuclease by aminoglycosides, RNA 8 (2002) 1393–1400.
[16] J. Åström, A. Åström, A. Virtanen, Properties of a HeLa cell 3' exonuclease specific for degrading poly(A) tails of mammalian mRNA, J. Biol. Chem. 267 (1992) 18154–18159.
[17] N.A. Balatsos, D. Anastasakis, C. Stathopoulos, Inhibition of human poly(A)-specific ribonuclease (PARN) by purine nucleotides: kinetic analysis, J. Enzym. Inhib. Med. Chem. 24 (2009) 516–523.
[18] N.A. Balatsos, D. Vlachakis, P. Maragozidis, S. Manta, D. Anastasakis, A. Kyritsis, M. Vlassi, D. Komiotis, C. Stathopoulos, Competitive inhibition of human poly(A)-specific ribonuclease (PARN) by synthetic fluoro-pyranosyl nucleosides, Biochemistry 48 (2009) 6044–6051.
[19] G. Gosselin, J.L. Girardet, C. Perigaud, S. Benzaria, I. Lefebvre, N. Schlienger, A. Pompon, J.L. Imbach, New insights regarding the potential of the pronucleotide approach in antiviral chemotherapy, Acta Biochim. Pol 43 (1996) 196–208.
[20] S. Manta, G. Agelis, T. Botic, A. Cencic, D. Komiotis, Fluoro-ketopyranosyl nucleosides: synthesis and biological evaluation of 3-fluoro-2-keto-beta-D-glucopyranosyl derivatives of N4-benzoyl cytosine, Bioorg. Med. Chem. 15 (2007) 980–987.
[21] W. Zhou, G. Gumina, Y. Chong, J. Wang, R.F. Schinazi, C.K. Chu, Synthesis, structure–activity relationships, and drug resistance of beta-d-3'-fluoro-2',3'-unsaturated nucleosides as anti-HIV Agents, J. Med. Chem. 47 (2004) 3399–3408.
[22] G. Agelis, N. Tzioumaki, T. Botic, A. Cencic, D. Komiotis, Exomethylene pyranonucleosides: efficient synthesis and biological evaluation of 1-(2,3,4-trideoxy-2-methylene-beta-d-glycero-hex-3-enopyranosyl)thymine, Bioorg. Med. Chem. 15 (2007) 5448–5456.
[23] G. Agelis, N. Tzioumaki, T. Tselios, T. Botic, A. Cencic, D. Komiotis, Synthesis and molecular modelling of unsaturated exomethylene pyranonucleoside analogues with antitumor and antiviral activities, Eur. J. Med. Chem. 43 (2008) 1366–1375.
[24] S. Manta, G. Agelis, T. Botic, A. Cencic, D. Komiotis, Unsaturated fluoro-ketopyranosyl nucleosides: synthesis and biological evaluation of 3-fluoro-4-keto-beta-d-glucopyranosyl derivatives of N(4)-benzoyl cytosine and N(6)-benzoyl adenine, Eur. J. Med. Chem. 43 (2008) 420–428.
[25] S. Manta, N. Tzioumaki, E. Tsoukala, A. Panagiotopoulou, M. Pelecanou, J. Balzarini, D. Komiotis, Unsaturated dideoxy fluoro-ketopyranosyl nucleosides as new cytostatic agents: a convenient synthesis of 2,6-dideoxy-3-fluoro-4-keto-beta-D-glucopyranosyl analogues of uracil, 5-fluorouracil, thymine, N4-benzoyl cytosine and N6-benzoyl adenine, Eur. J. Med. Chem. 44 (2009) 4764–4771.
[26] N. Tzioumaki, E. Tsoukala, S. Manta, G. Agelis, J. Balzarini, D. Komiotis, Synthesis, Antiviral and Cytostatic Evaluation of Unsaturated Exomethylene and Keto D-lyxopyranonucleoside Analogues, 342, Arch. Pharm., Weinheim, 2009, 353–360.
[27] P. Nilsson, A. Virtanen, Expression and purification of recombinant poly(A)-specific ribonuclease (PARN), Int. J. Biol. Macromol. 39 (2006) 95–99.
[28] Y. Cheng, W.F. Liu, Y.B. Yan, H.M. Zhou, A nonradioactive assay for poly(A)-specific ribonuclease activity by methylene blue colorimetry, Protein Pept. Lett. 13 (2006) 125–128.
[29] G.A. Kaminski, R.A. Friesner, J. Tirado-Rives, W.L. Jorgensen, Evaluation and reparametrization of the OPLS-AA force field for proteins via comparison with accurate quantum chemical calculations on peptide, J. Phys. Chem. B. 105 (2001) 6474–6487.
[30] R.A. Friesner, R.B. Murphy, M.P. Repasky, L.L. Frye, J.R. Greenwood, T.A. Halgren, P.C. Sanschagrin, D.T. Mainz, Extra precision glide: docking and scoring incorporating a model of hydrophobic enclosure for protein–ligand complexes, J. Med. Chem. 49 (2006) 6177–6196.
[31] N. Henriksson, P. Nilsson, M. Wu, H. Song, A. Virtanen, Recognition of adenosine residues by the active site of poly(A)-specific ribonuclease, J. Biol. Chem.285 (2010) 163–170.
[32] S.G. Waley, The kinetics of slow-binding and slow, tight-binding inhibition: the effects of substrate depletion, Biochem. J. 294 (Pt 1) (1993) 195–200.
[33] J.F. Morrison, C.T. Walsh, The behavior and significance of slow-binding enzyme inhibitors, Adv. Enzymol. Relat. Areas Mol. Biol. 61 (1988) 201–301.
[34] B. Perdicakis, H.J. Montgomery, J.G. Guillemette, E. Jervis, Analysis of slow-binding enzyme inhibitors at elevated enzyme concentrations, Anal. Biochem. 337 (2005) 211–223.
[35] S.E. Szedlacsek, R.G. Duggleby, Kinetics of slow and tight-binding inhibitors, Methods Enzymol. 249 (1995) 144–180.
[36] P.P. Shah, M.C. Myers, M.P. Beavers, J.E. Purvis, H. Jing, H.J. Grieser, E.R. Sharlow, A.D. Napper, D.M. Huryn, B.S. Cooperman, A.B. Smith 3rd, S.L. Diamond, Kinetic characterization and molecular docking of a novel, potent, and selective slow-binding inhibitor of human cathepsin L, Mol. Pharmacol. 74 (2008) 34–41.
[37] M.A. Xaplanteri, A.D. Petropoulos, G.P. Dinos, D.L. Kalpaxis, Localization of spermine binding sites in 23S rRNA by photoaffinity labeling: parsing the spermine contribution to ribosomal 50S subunit functions, Nucleic Acids Res. 33 (2005) 2792–2805.
[38] J. Martinez, Y.G. Ren, A.C. Thuresson, U. Hellman, J. Åström, A. Virtanen, A 54-kDa fragment of the poly(A)-specific ribonuclease is an oligomeric, processive, and cap-interacting poly(A)-specific 3' exonuclease, J. Biol. Chem. 275 (2000) 24222–24230.
[39] X. Zhang, A. Virtanen, F. E. Kleiman, To polyadenylate or to deadenylate: that is the question, Cell Cycle 9 4437–4449.
[40] J.W. Harper, S.J. Elledge, The DNA damage response: ten years after, Mol. Cell 28 (2007) 739–745.
[41] D.V. Bulavin, Y. Higashimoto, I.J. Popoff, W.A. Gaarde, V. Basrur, O. Potapova, E. Appella, A.J. Fornace Jr., Initiation of a G2/M checkpoint after ultraviolet radiation requires p38 kinase, Nature 411 (2001) 102–107.
[42] I.A. Manke, A. Nguyen, D. Lim, M.Q. Stewart, A.E. Elia, M.B. Yaffe, MAPKAP kinase-2 is a cell cycle checkpoint kinase that regulates the G2/M transition and S phase progression in response to UV irradiation, Mol. Cell 17 (2005) 37–48.
[43] H.C. Reinhardt, A.S. Aslanian, J.A. Lees, M.B. Yaffe, p53-Deficient cells rely on ATM- and ATR-mediated checkpoint signaling through the p38MAPK/MK2 pathway for survival after DNA damage, Cancer Cell 11 (2007) 175–189.
[44] M. Wu, M. Reuter, H. Lilie, Y. Liu, E. Wahle, H. Song, Structural insight into poly(A) binding and catalytic mechanism of human PARN, EMBO J. 24 (2005) 4082–4093.